High-sensitivity dispersive Mach–Zehnder interferometer based on a dissimilar-doping dual-core fiber for sensing applications

Hugo F. Martins,[1,2,4,*] J. Bierlich,[3] K. Wondraczek,[3] S. Unger,[3] J. Kobelke,[3] K. Schuster,[3] M. B. Marques,[1,2] M. Gonzalez-Herraez,[4] and O. Frazão[1,2]

[1]*INESC Porto, Rua do Campo Alegre, 687, 4169-007 Porto, Portugal*

[2]*Faculdade de Ciências da Universidade do Porto, Rua do Campo Alegre, 687, 4169 007 Porto, Portugal*

[3]*Leibniz Institute of Photonic Technology (IPHT Jena), Albert-Einstein-Strasse 9, 07745 Jena, Germany*

[4]*Departamento de Electrónica, Universidad de Alcalá, Escuela Politécnica DO-231, 28871 Spain*

**Corresponding author: hfm@inescporto.pt*

Received March 4, 2014; accepted March 27, 2014;
posted April 2, 2014 (Doc. ID 207679); published April 30, 2014

A dual-core fiber in which one of the cores is doped with germanium and the other with phosphorus is used as an in-line Mach–Zehnder dispersive interferometer. By ensuring an equal length but with different dispersion dependencies in the interferometer arms (the two cores), high-sensitivity strain and temperature sensing are achieved. Opposite sensitivities for high and low wavelength peaks were also demonstrated when strain and temperature was applied. To our knowledge this is the first time that such behavior is demonstrated using this type of in-line interferometer based on a dual-core fiber. A sensitivity of (0.102 ± 0.002) nm/με, between 0 *and* 800 με and (-4.2 ± 0.2) nm/°C between 47°C and 62°C is demonstrated.

OCIS codes: (060.2370) Fiber optics sensors; (060.2310) Fiber optics; (060.4005) Microstructured fibers.
http://dx.doi.org/10.1364/OL.39.002763

Dual-core, or two-core, fibers were first proposed as strain sensors in 1981 [1]. These types of fibers were also demonstrated as temperature sensors in 1983 [2]. With the advent of microstructured fibers, several dual-core fibers were developed, such as twin-core fibers with special air cladding [3], based on photonic bandgap fibers [4,5] and polymer fibers [6]. Hybrid dual-core fibers where light is guided by total internal reflection in one core and by bandgap guidance in the other were also proposed for wavelength-selective coupling [7]. More recently, another type of microstructured dual-core fiber was developed: the suspended twin-core fiber. In this case the two cores appear to be suspended in large air holes by thin glass bridges [8]. All these configurations can be used for the measurement of different parameters, such as refractive index [5,9,10] or biosensing [6]. Through the selective infiltration of a single hole with fluid along a dual-core photonic crystal fiber (PCF), a record sensitivity for a fiber device of 30,100 nm per refractive index unit was demonstrated [10].

Usually, when the Mach–Zenhder (MZ) interferometer is subjected to physical parameter, the phase changes as the length or/and the refractive index is altered in one of the arms. The main advantage of using a single fiber with twin-cores is the stability of the interferometer, namely with the temperature. Strong immunity to bending has also been demonstrated using a twin-core PCF for an in-line MZ interferometer [11]. However, by designing the fiber to have two different cores, it can be made highly sensitive to these parameters. The design of the fiber also introduces relevant trade-offs: the optical coupling between the two cores can be a limitation when the two cores are close [6]. On the contrary, when the two cores are very distant, coupling light simultaneously from a single-mode fiber (SMF) to the two cores may be challenging. In this case to solve the problem, a tapered fiber splice is a convenient solution.

In this Letter, the authors present an in-line dispersive MZ interferometer based on a dissimilar dual-core fiber used as a sensing element. The optical path is different because the two cores present different doping materials (and hence different refractive indices and different sensitivities to strain and temperature). The dispersive interferometer is characterized in strain and temperature and demonstrated to be an alternative solution for high-sensitivity measurement of these magnitudes.

The dual-core fiber used as sensing device had a length of 0.5 m and measured losses of ~15 dB/km at 1550 nm. The host material of the fiber was pure silica and the diameter of the cladding was 125 μm. As for the cores, one of them was doped with germanium, had a diameter of 5.1 μm, an expected Δn of 0.013 (estimated from the fiber preform), and a NA of 0.195. The second core was doped with phosphorous, had a diameter of 6.4 μm, a Δn of 0.00835, and a NA of 0.155.

The core sizes were chosen in order to achieve an estimated cutoff wavelength of ~1.3 μm in both cores. The distance between the two cores was approximately 14.9 μm, thus strongly reducing cross talk between the two cores [6]. An image of the transversal cross section of the dual-core fiber geometry is presented in Fig. 1.

First, a theoretical model for the dispersive interferometer is developed. The interferometer is created by splicing both ends of the dual-core fiber with standard SMF. Since the two cores of the dual-core fiber have different refractive indices, these will present different optical paths and an interferometer is created. When strain or temperature is applied to the dual-core fiber, the optical path difference between the interferometer arms (the two cores) is changed, and therefore the optical spectrum at the end of the interferometer is changed. Since

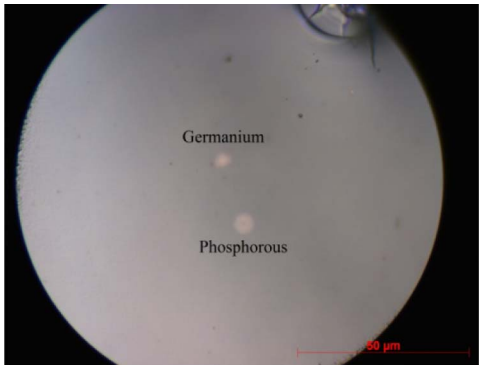

Fig. 1. Cross section of the dual-core fiber, showing the germanium- and phosphorous-doped cores.

the two cores are built in the same silica matrix, the arms of the interferometer are assumed to always have the same length. This is a key aspect of the dual-core fiber-based MZ interferometer. In traditional MZ interferometers, a change in the length of an arm will change the phase by a factor proportional to the refractive index of the arms (n_1, n_2). In this case, however, a change in the fiber length will only change the phase by a factor proportional to the difference of refractive index among the two cores $(\Delta n = n_1 - n_2)$, which is much smaller than n_1, n_2. At the end of the dual-core fiber, the light in the core i will be given by

$$\vec{E}_i(\omega) = \vec{E}_i \cdot e^{j(L \cdot k_i(\omega) + \phi_0)}, \tag{1}$$

where E_i is the amplitude of the field of the core i $(i = 1, 2)$, L is the fiber length, and $k(\omega)_i$ is the wavenumber of the core i, which is a function dependent on the angular frequency (ω). Although some degree of birefringence must also exist in this type of fiber, a simple analysis allows concluding that for the number of fringes observed, the birefringence does not play an important role and is therefore neglected. Birefringence would essentially result in the sum of two interferometers (the fast and slow axis of the cores), which would add an envelope function after a large number of fringes. The intensity of the light at the end of the dual-core fiber (sum of the fields coming from cores 1 and core 2) will be given by

$$I_{\text{out}}(\omega) = I_1 + I_2 + 2\sqrt{I_1 I_2}\,\cos[L \cdot \Delta k(\omega)], \tag{2}$$

where $\Delta k(\omega) = k_1(\omega) - k_2(\omega)$. In this case, the evolution of the interference fringes of the dispersive interferometer will be determined by the argument of the cosine, hereinafter referred as the phase of the interferometer [Phase(ω)]. When Phase(ω) has a value of $m * 2\pi$ $(m * 2\pi + \pi)$, where m is an integer, the interference spectrum has a local maximum (minimum). Using the Taylor expansion of $\Delta k(\omega)$ around an arbitrary ω_0 we obtain

$$\Delta k(\omega) = \Delta k(\omega_0) + (\omega - \omega_0)\frac{\partial \Delta k}{\partial \omega}\bigg|_{\omega_0} + (\omega - \omega_0)^2 \frac{1}{2}\frac{\partial^2 \Delta k}{\partial \omega^2}\bigg|_{\omega_0} + \ldots, \tag{3}$$

where $d\Delta k(\omega)/d\omega$ is the difference between the inverses of the group velocities of cores 1 and 2 in ω_0 and $d^2\Delta k(\omega)/d\omega^2$ is the difference between the group delay dispersions (ΔGDD) of cores 1 and 2 in ω_0. Dispersion terms of order higher than 2 are neglected as the frequency range used in the experimental measurements is not very large. In conventional MZ interferometers based on twin-core fibers, the dispersion difference among the cores can be considered very low. Here, the fiber is actually composed of two cores with highly dissimilar dopings (Ge and P). This leads to an interesting dispersion change of the interferometer around 1550 nm, which makes it especially sensitive. In the experimental measurements it was observed that there is a point in which Phase(ω) remains constant for variations of ω. For simplicity, we define ω_0 as this point and therefore $d\Delta k(\omega)/d\omega$ equals zero in ω_0. Under these conditions, Phase(ω) will be a quadratic function with center in ω_0. Figure 2 shows three theoretical plots of Phase$(\omega)/2\pi$ as a function of wavelength (λ) (using $\lambda = 2\pi c/\omega$) under different conditions, which are compared with the experimental measurements. The line (a) shows the theoretical (and experimental) peak values obtained for the unstrained fiber at room temperature In this case, the values used were: $L = 0.5$ m, $\Delta k(\omega_0) = 2\pi\Delta n_0/\lambda_0$, $\omega_0 = 2\pi c/\lambda_0$ where c is the velocity of light in the vacuum, $\lambda_0 = 1540$ nm the central wavelength in the vacuum, and $\Delta n_0 = 0.0046559$. For the case (b) where temperature was applied to the fiber (50°C shift), the used values were $L = 0.5000125$ m (the modified length was obtained using a coefficient of thermal expansion for silica of $\approx 10^{-6}$/°C), $\lambda_0 = 1553$ nm and $\Delta n_0 = 0.0047325$, and for the case (c) where strain was applied to the fiber (1000 με) the used values were $L = 0.5005$ m, $\lambda_0 = 1533$ nm, and $\Delta n_0 = 0.0046079$. In all cases, a value of ΔGDD $= 22$ fs^2/mm [difference of dispersion parameter between the cores $=$ 41.4 ps/(nm.km)] was used and a good agreement was observed between the theoretical (when Phase$(\lambda)/2\pi =$ integer) and experimental (dots of the graphic) peaks of the interferometer. With an increase/decrease of the Δn_0

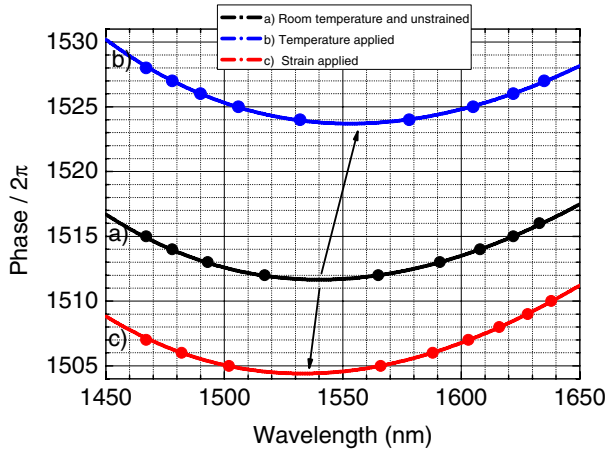

Fig. 2. Theoretical phase (the lines) of the interferometer as a function of the wavelength for fiber at (a) room temperature with no strain, (b) temperature applied, (c) strain applied. The experimental peaks are also represented (dots). The values used in the simulation are presented in the text.

the value of Phase(ω) increases/decreases, causing the peaks to move toward/away from the center of the dispersion interferometer (λ_0). In the simulations it was possible to observe that changes in Δn_0 of 10^{-6} caused substantial (>1 nm) changes in the peaks positions. Equivalent variations in the peaks positions were only achieved in the simulation with changes of $\Delta L > 1000$ με (with $\Delta n_0 =$ constant). In this case, it is expected that when straining the fiber, the impact of the stress-optic coefficient will be higher than the impact of the fiber length increase, as demonstrated in the experimental results.

Figure 3 presents the experimental configuration used to characterize the dispersion interferometer based in a dual-core fiber as sensing element. The dispersive interferometer is created by splicing both ends of the dual-core fiber with SMF. The core of the SMF was placed between the two cores, thus minimizing the differences between the amount of light coupled into each of the cores and therefore increasing the visibility. After the fusion splice, the fiber is tapered reducing the diameter of the fiber in the splice region to ≈60 μm (approximately half the initial size). This increases the NA and therefore the coupling of light into both cores. Strain was applied to the dual-core fiber by fixing one end to a stationary stage and the other end to a micrometric translation stage on which deformations were applied at 13°C. As for the temperature measurements they were performed with no strain applied to the dual-core fiber. An erbium-doped fiber amplifier (EDFA) was used to illuminate the dispersive interferometer and an optical spectrum analyzer (OSA) with a maximum resolution of 0.01 nm was used to interrogate it in transmission.

Figure 4 presents the transmission spectrum of the dispersive interferometer and the respective wavelength shift for increasing applied strain [Fig. 4(a)] and temperature [Fig. 4(b)]. The characteristic dips of an interferometer appear in the spectral response as expected. The spacing between the dips presents symmetry around a central wavelength (at ≈1540 nm) and decreases when moving away from it. In terms of sensitivity (both to strain and temperature), the interferometer peaks present opposite response for wavelengths higher and lower than the central wavelength. These peaks move symmetrically away/toward the center for applied strain/temperature, as predicted by the theoretical model. To our knowledge this is the first time that this effect is observed in this type of in-line interferometer based on a dual-core fiber. As explained in the theoretical model, this is owed to a change in the sign of the derivative of $\Delta k(\omega)$. The visibility of the peaks seems to

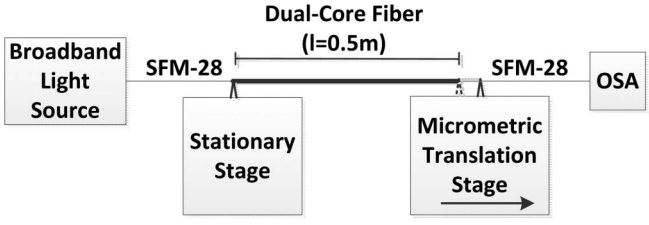

Fig. 3. Experimental setup used to characterize the dual-core fiber as a strain and temperature sensor.

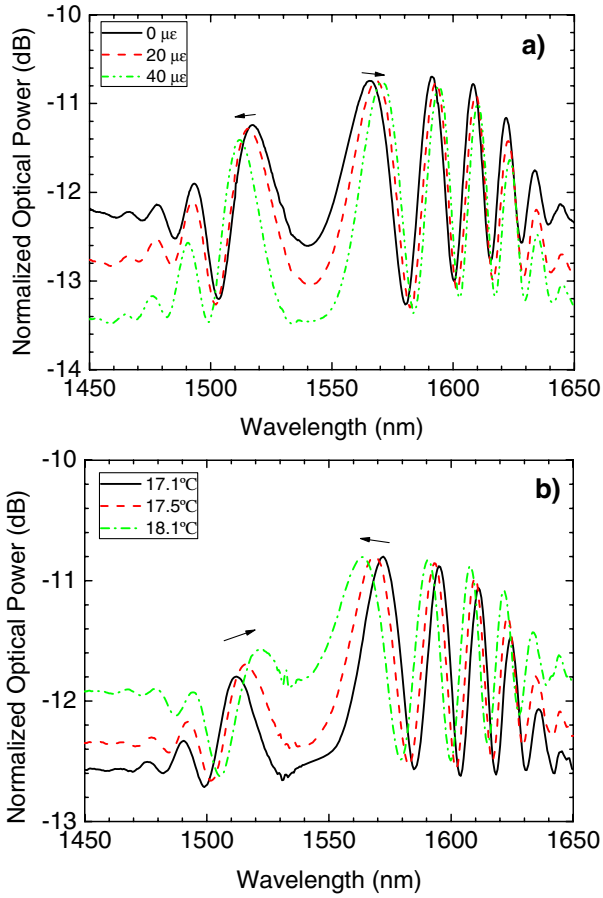

Fig. 4. Shift of the normalized transmission spectrum of the dispersive interferometer with increasing applied (a) strain and (b) temperature.

decrease when moving away from the center. This effect, however, is owed to the emission spectrum of the EDFA, which transmits more light in the 1500–1600 nm range than in the rest of the observed range. When observed with a broader light source, the peaks presented similar visibilities in a higher range (at least 1400–1700 nm).

Figure 5 shows the wavelength shift of the peaks of the dispersive interferometer spectrum when (a) strain (at 13°C) and (b) temperature (with no strain) is applied.

With increasing applied strain [Fig. 5(a)] the interference fringes are observed to move toward the center. Given the parabolic nature of the evolution of Phase(λ), the sensitivity of the peaks decreases when moving away from the center. Monitoring a single peak, average sensitivities of (-0.125 ± 0.003) nm/με (1520–1460 nm) and (0.102 ± 0.002) nm/με (1540–1640 nm) were observed when a strain of up to 800 με was applied. This value is much higher than the typical values presented by fiber Bragg based sensors (≈1 pm/με [12]) or traditional dual-core in-line MZ interferometers (≈1 pm/με [11,13]), in which the difference between dispersion dependencies of the two cores is much weaker than the ones presented in this work.

As for the temperature measurements, with increasing applied temperature [Fig. 5(b)] the interference fringes are observed to move away from the center. Monitoring a single peak, average sensitivities of (-4.0 ± 0.1) nm/°C

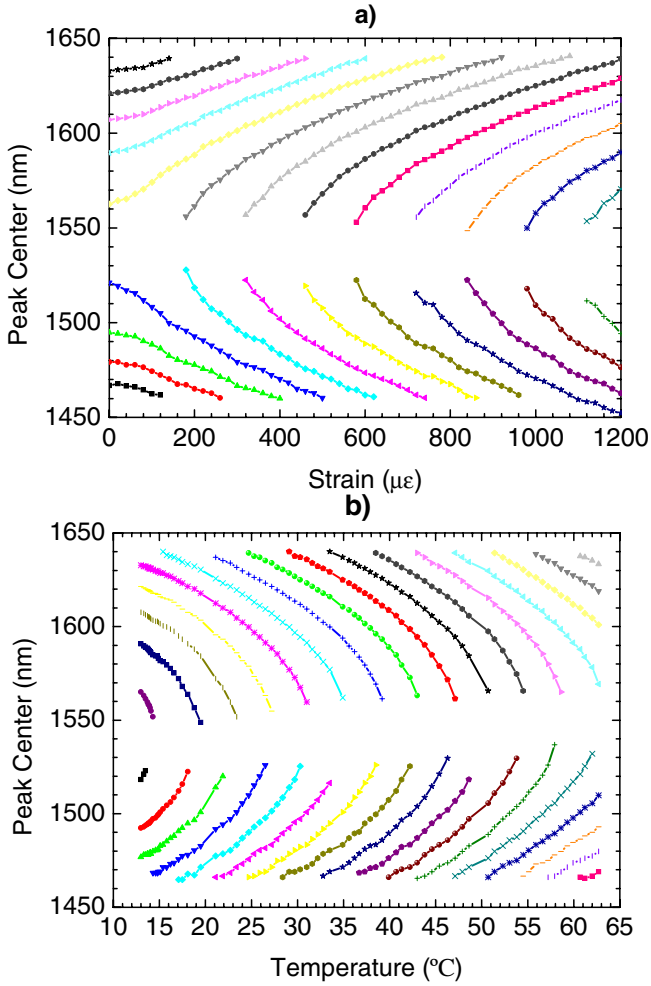

Fig. 5. Peaks wavelength shift of the dispersive interferometer spectrum as function of the applied (a) strain and (b) temperature.

(1640–1570 nm) and (4.2 ± 0.1) nm/°C (1460–1540 nm) were observed when the temperature was raised from 47°C to 62°C. In this case, taking the resolution of the OSA (0.01 nm) a resolution of the experimental setup of 0.002 με and 0.08°C can be estimated.

It is also important to point out that the center of the spectrum ($\Delta k(\omega) = 0$) was observed to shift ≈ -7 nm from 1540 to 1533 nm, while maintaining the form of the transmission spectrum, for an applied strain between 0 *and* 1000 με [Fig. 5(a)] and ≈13 nm (from 1540 to 1553 nm) when the temperature was raised from 13°C to 62°C [Fig. 5(b)]. This means that the dispersion curve was changed when applying temperature/strain. This effect can be used to measure the value of the absolute temperature/strain rather than only measuring variations of temperature/strain.

In conclusion, a new device concept for a highly sensitive MZ interferometer, based on a dual-core fiber with dissimilar-doping is described theoretically and experimentally. By ensuring the same length in both arms of the interferometer (built in the same silica matrix), the interferometer is only sensitive to the variations in differential dispersion among the two cores, thus allowing high-sensitivity strain and temperature sensing with also a good robustness and even potential for absolute measurements.

A theoretical model is given presenting good agreement with the experimental results. Opposite sensitivities for wavelength peaks higher and lower than the central wavelength of the interferometer were demonstrated when strain and temperature were applied. To our knowledge this is the first time that such behavior is demonstrated using this type of in-line interferometer based on a dual-core fiber. The effect is demonstrated to be owed to a sign reversal in differential dispersion between the wavenumbers of the cores.

A sensitivity of (0.102 ± 0.002) nm/με, between 0 *and* 800 με and (-4.0 ± 0.2) nm/°C between 47°C and 62°C is demonstrated. The center of the spectrum was observed to shift to higher/lower wavelengths with applied temperature/strain, which allows the measurement of absolute temperature/strain.

This work was supported by project "NORTE-07-0124-FEDER-000058," which is financed by the North Portugal Regional Operational Programme (ON.2–O Novo Norte), under the National Strategic Reference Framework (NSRF) through the European Regional Development Fund (ERDF); by Portuguese national funds, through a bilateral cooperation between the Portuguese funding agency Fundação para a Ciência e a Tecnologia (FCT) and DAAD; by funding from the European Research Council through Starting Grant U-FINE (grant 307441); and by the Spanish "Plan Nacional de I+D+i" through project TEC2012-37958-C02-01. H. Martins acknowledges a scholarship from FCT Fundação para a Ciência e a Tecnologia (Portuguese Foundation for Science and Technology), SFRH/BD/76991/2011.

References

1. G. Meltz and E. Snitzer, "Fiber optic strain sensor," WIPO patent WO1981000618 A1 (March 5, 1981).
2. G. Meltz, J. R. Dunphy, W. W. Morey, and E. Snitzer, Appl. Opt. **22**, 464 (1983).
3. L. Zhang and C. Yang, J. Lightwave Technol. **22**, 1367 (2004).
4. Z. Wang, T. Taru, T. A. Birks, J. C. Knight, Y. Liu, and J. Du, Opt. Express **15**, 4795 (2007).
5. W. Yuan, G. E. Town, and O. Bang, IEEE Sens. J. **10**, 1192 (2010).
6. C. Markos, W. Yuan, K. Vlachos, G. E. Town, and O. Bang, Opt. Express **19**, 7790 (2011).
7. X. Sun, Opt. Lett. **32**, 2484 (2007).
8. O. Frazão, R. M. Silva, J. Kobelke, and K. Schuster, Opt. Lett. **35**, 2777 (2010).
9. G. Town, W. Yuan, R. McCosker, and O. Bang, Opt. Lett. **35**, 856 (2010).
10. D. Wu, B. Kuhlmey, and B. Eggleton, Opt. Lett. **34**, 322 (2009).
11. B. Kim, T. Kim, L. Cui, and Y. Chung, Opt. Express **17**, 15502 (2009).
12. H. F. Martins, M. B. Marques, and O. Frazão, Appl. Phys. B **104**, 957 (2011).
13. S. Liu, N. Liu, Y. Wang, J. Guo, Z. Li, and P. Lu, IEEE Photon. Technol. Lett. **24**, 1768 (2012).